LASER INTERFEROMETER GRAVITATIONAL WAVE OBSERVATORY
- LIGO -
CALIFORNIA INSTITUTE OF TECHNOLOGY
MASSACHUSETTS INSTITUTE OF TECHNOLOGY

Technical Note **LIGO-T1000075–v2** 2010/07/18

Advanced Interferometer Configurations White Paper: Beyond the Second Generation

Yanbei Chen and Rana Adhikari

Distribution of this document:
AIC, ISC

California Institute of Technology
LIGO Project, MS 18-34
Pasadena, CA 91125
Phone (626) 395-2129
Fax (626) 304-9834
E-mail: info@ligo.caltech.edu

Massachusetts Institute of Technology
LIGO Project, Room NW22-295
Cambridge, MA 02139
Phone (617) 253-4824
Fax (617) 253-7014
E-mail: info@ligo.mit.edu

LIGO Hanford Observatory
Route 10, Mile Marker 2
Richland, WA 99352
Phone (509) 372-8106
Fax (509) 372-8137
E-mail: info@ligo.caltech.edu

LIGO Livingston Observatory
19100 LIGO Lane
Livingston, LA 70754
Phone (225) 686-3100
Fax (225) 686-7189
E-mail: info@ligo.caltech.edu

http://www.ligo.caltech.edu/

Contents

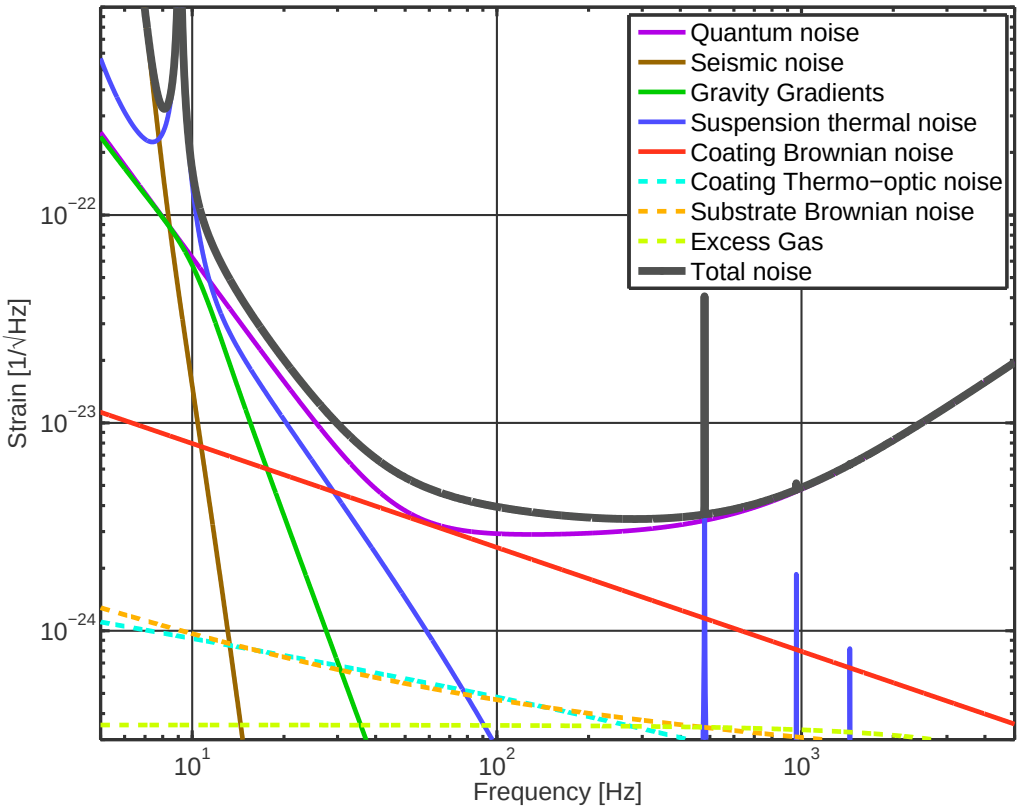

Figure 1: Baseline AdL Noise Budget via GWINC v2.0. Power into the interferometer is 125 W. Arm cavity power is 730 kW. SRM position is tuned to 0 deg for broadband operation.

1 Introduction

The aim of the AIC Working Group is to carry out theoretical and experimental research for both short- and long-term upgrades/re-designs of ground-based gravitational-wave detectors. In this White Paper, we summarize a list of topics that will define the scope of research in our Working Group.

The core interest of the group is "the optical configuration", namely the design of the idealized device that only includes the longitudinal optical mode and the translational mechanical modes. It is this device that interacts directly with the incoming gravitational wave, and determines an idealized noise spectrum for the entire interferometer. However, this idealized interferometer only exists as part of a larger system, the entire interferometer. Our idealized interferometer suffers from constraints imposed by design limitations of the entire interferometer (e.g., mass of mirrors, optical power, pendulum frequency etc.), and from residual coupling with other degrees of freedom. This coupling can be linear, and result in additional noise (e.g., laser noise, internal/suspension thermal noise, seismic noise, etc.); it can also be nonlinear, and result in a modification of dynamics, causing instabilities (e.g., tilt instabilities).

As a consequence, design of the idealized interferometer must be an interactive one, with other effects in mind. To be concrete, we divide our efforts into two parts: those involving an upgrade to Advanced LIGO (LIGO 2.5), and those towards third-generation detectors

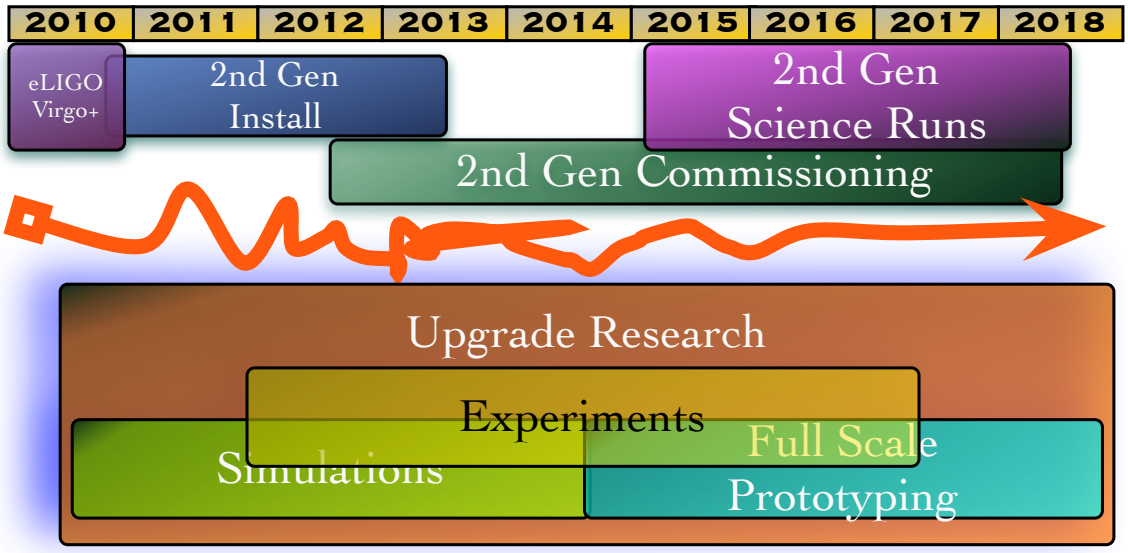

Figure 2: Timeline for Research into post 2nd gen Upgrades

(LIGO 3). [1]

- For *LIGO 2.5*, we have a more concrete time line, with the aim of deployment starting from 2016. IF we imagine it to be similar to the LIGO 1.5 upgrade it would be required to be a modest upgrade (3 years / 50 million USD). This means we need to set our design within a constraint that is regarded as realistic for that time scale.
- For *LIGO 3*, designs of optical configurations with better sensitivity can help identify the particular need to improve certain areas. For example, the use of squeezed vacuum (especially if the Standard Quantum Limit were to be surpassed) may require a much more stringent tolerance to optical mode matching and optical losses.

2 Constraints

In this section, we identify, or rather, outline a program that identifies the constraints applicable to LIGO 2.5 and LIGO 3, respectively.

2.1 LIGO 2.5

In the LIGO 2.5 timescale, we mainly need to design optical configurations geared toward concrete constraints from somewhat reliable projections of other technical constraints. To be ready $\sim$ 2016, we would need to have the laboratory scale R&D begin within 1 year or

[1] The numbering here to distinguish Advanced LIGO upgrades from 3rd generation interferometers is just here for clarity. It is not within the scope of AIC to decide on the various permututations of Enhanced, Advanced, Super-duper, Wonderful, Ultimate, etc.

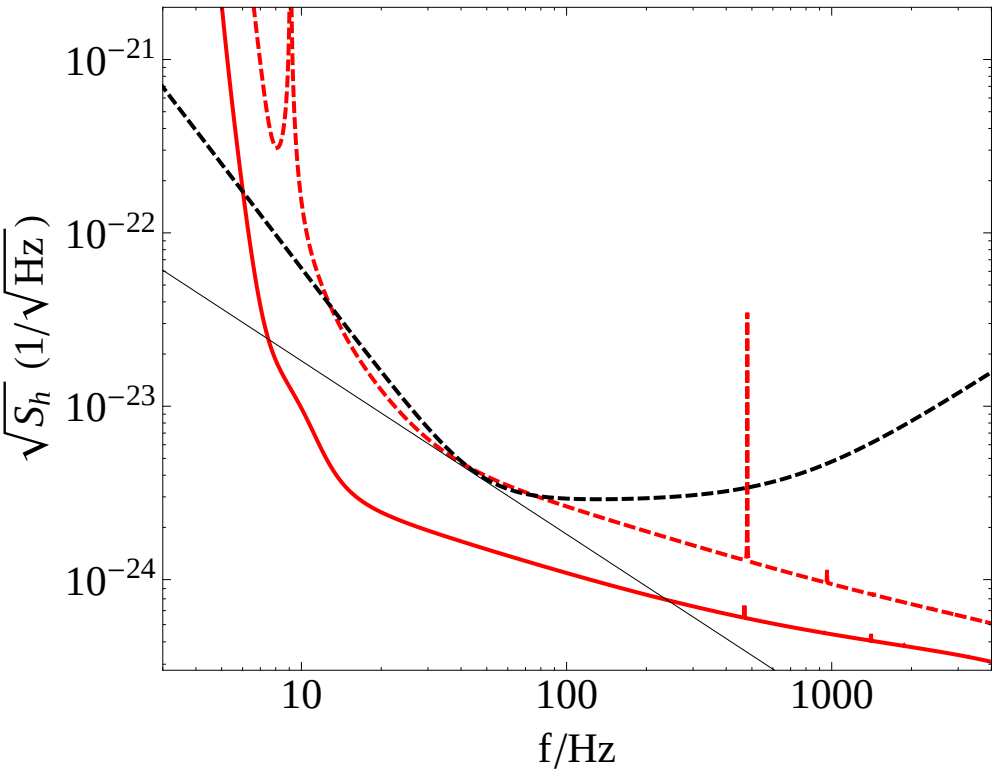

Figure 3: Total non-optical noise spectrum of LIGO 2.5 (red solid), as assumed in Sec. 2.1, in comparison with the corresponding curve of Advanced LIGO (red dashed), as well as (broadband) quantum noise of Advanced LIGO baseline (black dashed).

so. Of course, its difficult to know exactly what upgrades will be most beneficial before the commissioning of Advanced LIGO reveals the problems. Lacking this knowledge, we can instead choose to develop those technologies that will produce a significant improvement in only the known limiting noise sources.

1. We may expect coating thermal noise and suspension thermal noise to moderately improve, and therefore leaving space for sensitivity improvement in the $5 - 50$ Hz range. These require improvements in the test mass coating technology (e.g. materials) and upgrades of the suspension system. At the moment, it is important to push a research program that deals with thermal noise improvement. We need to have a clear idea of the plausible improvement rather soon. For the purposes of proceeding with the optical design we will assume an improvement of a factor of 2 in the coating Brownian noise amplitude spectral density (factor of 4 in the power spectrum). For some related technologies see the Appendix.

2. For the suspension thermal noise, will assume that the bounce mode frequency can be lowered by a factor of 3 with a concomitant reduction in the vertical mode thermal noise. (See Appendix B)

3. We will not consider major changes in the facility, nor can we significantly modify the mirror size. We also rule out cryogenic mirrors in this time frame.

4. It is possible that Newtonian noise mitigation through active noise cancellation would become realistic during this time scale. Therefore we assume a reduction by a factor of 10 of the Newtonian noise.

5. We may be able to modify the configuration by modifying the signal recycling cavity, possibly by elongating the cavity into 4 km. (See Sec. 3.3).

6. There are optical configurations allowing the injection of squeezing, which may be filtered by cavities with moderate lengths (10's of meters), or even 4 km. (See Sec. 3.1; for generating squeezing using small interferometers instead of nonlinear optical medium, see Sec. 3.6)

7. It may be possible to inject multiple carrier frequencies into the interferometer in order to shape the frequency response or to provide alternative means for controlling the length and alignment degrees of freedom. (See Sec. 3.4)

Modeling activities involving these aspects should be completed within a few years, and should pay special attention to practical imperfections, and sensing/control issues. In Figure 3, we plot the non-optical noise spectrum of Advanced LIGO (red dashed curve), the Advanced LIGO quantum noise (broadband configuration, black dashed curve), and the total non-optical noise spectrum of LIGO 2.5 that corresponds to the above discussions (red solid curve).

2.2 LIGO 3

For LIGO 3, the constraints are less concrete, yet they certainly allow more dramatic improvement of sensitivity.

One of the major decisions affecting the design will be whether or not the 3rd generation interferometers are built underground. There are pros and cons to underground interferometers and we need to do a design study to compare the sensitivity of underground interferometers with ones utilizing the existing LIGO facilities.

1. System considerations. We need to explore different interferometer geometry.
2. We need to identify the potential for each of the critical technical aspects.
   (a) How big can the mirrors / test masses be? Can large masses be supported by the suspension?
   (b) How much lower can thermal noise in the coating/substrate be? Cryogenics? How?
   (c) What can we expect for suspension thermal noise? Cryogenic fibers? Magnetic suspensions?
   (d) What is the ultimate amount of power we can have / handle?
   (e) What may be the level of Newtonian noise on the surface after subtraction? Underground?
   (f) Can the gas damping be sufficiently mitigated in the future suspension design?
   (g) Can atoms be added? What about Noise?

In planning third-generation detectors, we must also consider the astrophysical motivation. For example, for a particular candidate population, we need to seek as information as to the possible gain of scientific pay-off corresponding to particular improvements of sensitivity.

3 Interferometer Topology Options

3.1 Optical Filtering and Strategies for Injecting Squeezing

3.1.1 Phase and Amplitude Filters

Optical filters have been designed to take advantage injected squeezing, as well as adapting optimally to ponderomotive squeezing (i.e., squeezing generated internally in the interferometer), and achieving so-called back-action evasion. The use of input squeezing to improve interferometer sensitivity originated from works of Unruh and Caves [22, 23], which considered frequency independent squeezing. The use of optical filters to achieve back-action evasion originated from the variational readout strategy by Vyatchanin et al. in the time domain [24], which considered the varying readout quadrature in time. The filters we discuss here can rotate quadratures according to sideband frequency, and are best adapted for use in LIGO:

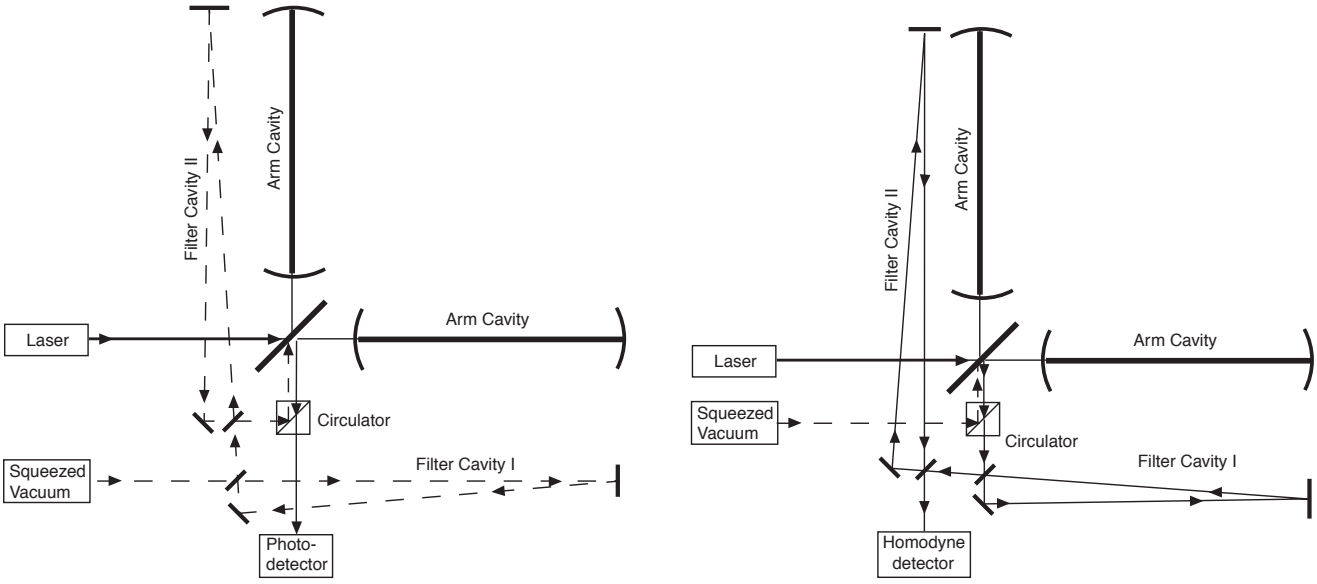

Figure 4: Frequency dependent input squeezing (left panel) and Frequency dependent homodyne detection (right panel) with optical filters. [Adapted from Kimble et al. [25].]

- Kimble et al. [25] designed Fabry-Perot cavity filters (with one coupling mirror and perfect end mirror) for optimal squeezing injection, as well as optimal readout, in broadband Fabry-Perot Michelson interferometers (see Fig. 4 for layout of these configurations, as well as left panel of Fig. 5 for an individual filter). These filters achieve their goals by rotating quadratures in a frequency dependent manner. Kimble et al.'s filter design strategy (including the use of successive Kimble filters) is generalized by Purdue and Chen [17] into general quadrature rotation angles.

- Harms et al. [26], Buonanno and Chen [27], generalized Kimble filters to detuned signal recycling. They obtained the optimal filter for injecting frequency-dependent squeezing and detecting constant homodyne phase. They also obtained the optimal frequency dependence of homodyne detection, yet failed to find filters that realize such angles.

- Corbitt et al. designed *amplitude filters* [28], which are made up from impedance-matched cavities: either amplitude or phase squeezing is injected into the interferometer, with a different *portion*, depending on the frequency. (See right panel of Fig. 5.) They also considered serial and parallel amplitude filters.

- Khalili [29] substantially improved the amplitude filter by adding a homodyne detection at the open port — and subtracting this channel from the main detection channel with the appropriate gain. (See right panel of Fig. 5.) This was further developed [30].

In general, input squeezing combined with output filtering, in idealized situations, can totally eliminate radiation-pressure noise, and suppress shot noise by the squeeze factor. Input squeezing combined with input filtering, on the other hand, does not eliminate radiation-pressure noise, but simply suppress shot noise and radiation-pressure noise by the squeeze factor.

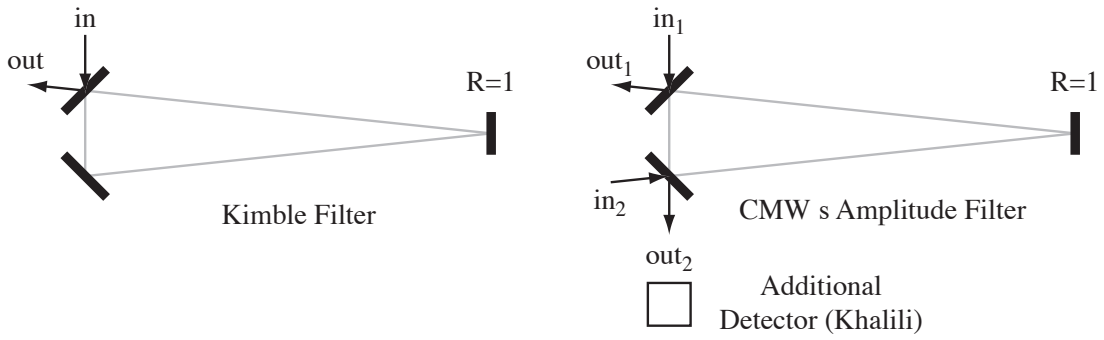

Figure 5: Left Panel: Kimble filters, with only one input and one output. Right Panel: Amplitude Filter proposed by Corbitt Mavalvala and Whitcomb, and improved by Khalili, who proposed adding an additional homodyne detection.

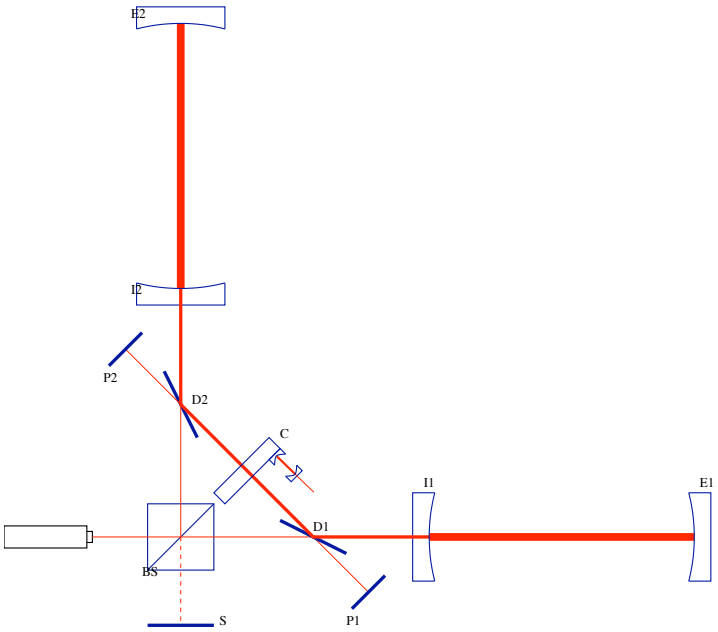

Figure 6: Interferometer with an intracavity readout scheme, taken from Ref. [36]

However, the advantage of output filtering is achieved by utilizing the ponderomotive squeezing generated inside the interferometer, which requires measuring output quadratures with low signal strength. As a consequence, output filtering is much susceptible to optical losses.

3.1.2 Loss Limitation

Optical losses might become more important when squeezing is used, or when internal ponderomotive squeezing is employed for sensitivity improvement (e.g. in schemes with output filtering).

The effect of losses is further amplified if back-action evasion is required, in which case the signal strength in the quadrature being detected is significantly less than conventional situations. A rule of thumb for this limitation is available from Kimble et al. [25], where we have

$$\sqrt{S_h/S_h^{\mathrm{SQL}}} \geq (e^{-2q}\mathcal{E})^{-1/4} \tag{1}$$

where $\mathcal{E}$ is the power loss, and e^{-2q} is the power squeezing factor. Assuming $\mathcal{E}$ to be 0.01, and 10 dB squeezing, we have a SQL-beating limit of 0.18.

For a given filter bandwidth γ_{filter} (to be determined by the needs of input/output filtering), when realized by a cavity of length L, the total loss $\mathcal{E}$ is determined by

$$\mathcal{E} = \frac{4\epsilon}{T} = \frac{\epsilon c}{\gamma_{\mathrm{filter}} L} \tag{2}$$

where T is the input-mirror power transmissivity [related to bandwidth by $\gamma_{\mathrm{filter}} = Tc/(4L)$] and ϵ is the loss per round-trip. It is therefore the ratio ϵ/L that determines the goodness of the filter. Since the per-round-trip loss ϵ depends on the beam spot size, which in turn depends on L, an optimization is need to find out the optimal length and design of filter cavities [31].

Practically speaking, ultra-low losses (around 1 ppm) have been achieved on the mirrors of fixed cavities [19, 20]. However, the lowest loss measured on the large, test-mass-sized beams are more usually in the 50-100 ppm range. FFT simulations have shown that the loss for large beams is dominated by the large scale figure error of the substrate, while the losses for small beams are dominated by point defects in the coatings. Since the low frequency performance of the QND schemes so strongly depends on the loss for intermediate sized ($\sim$mm) beams, it is vitally important to develop ultra-low loss mirrors for this beam size. The modern polishing technology is already good enough.

3.2 Time-dependent Homodyne Detection

In a detuned interferometer, the GW signal appears in both quadratures of the output electric field. The sensitivity of interferometer can be shaped by measuring a frequency dependent combination of these quadratures (as in GEO600), but also by having the measured quadrature be a *time dependent quantity*. For example, this could be done by varying the phase of the LO field used to do the signal extraction.

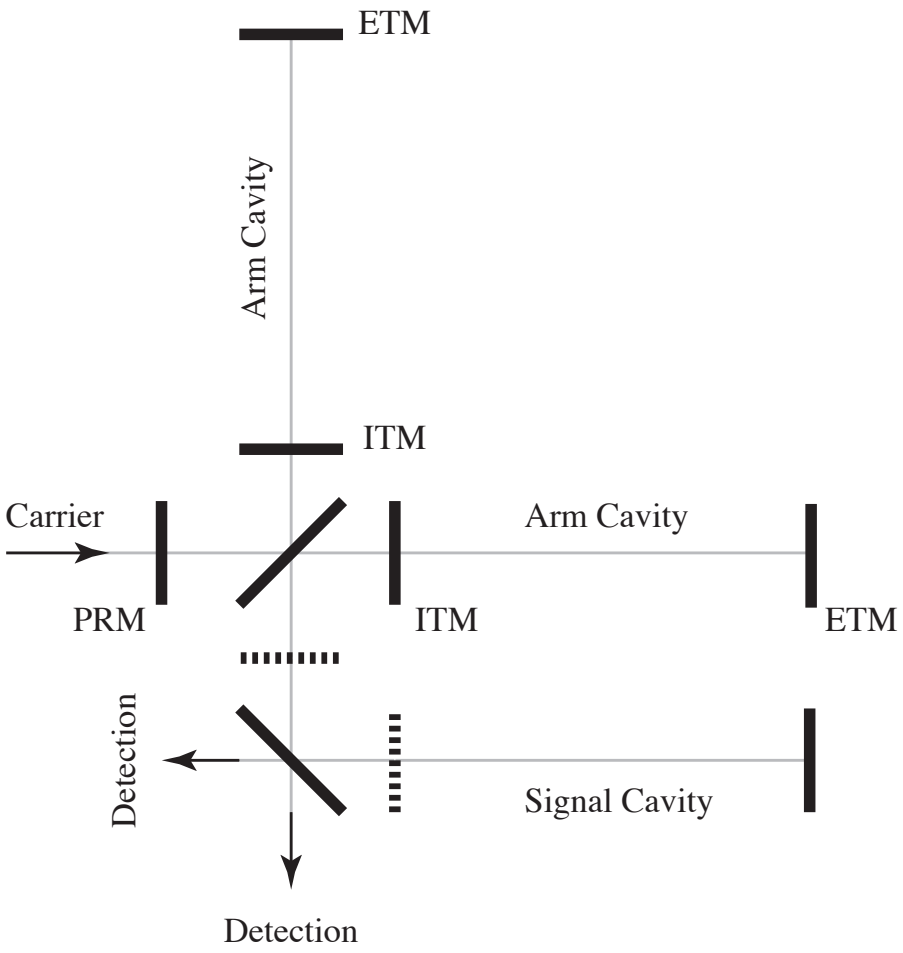

Figure 7: Fabry-Perot Michelson interferometer with long signal recycling cavity. Dashed lines indicate possible positions of signal-recycling mirrors.

3.3 Modifications to the Signal Recycling Cavity

3.3.1 Variable Reflectivity Signal Mirror

The signal recycling mirror can be replaced with a Fabry-Perot cavity. This tunable cavity will change the effective reflectivity of the signal mirror and allow for a tunable finesse for the signal cavity in addition to the usual signal cavity detuning phase. This can be realized either by an etalon, or by a Michelson interferometer, as has been demonstrated at the ANU [15]. This option is also naturally combined with the concept of a long signal recycling cavity.

3.3.2 Long Signal Recycling Cavity

The Advanced LIGO signal cavity is designed to be $\simeq 50$ m. It will be possible to extend this cavity to 4 km, as shown in Fig. 7. A long signal-recycling cavity has been shown to be advantageous in that it is non-degenerate [1]. In addition, long SR cavities has been shown to be interesting in the following ways.

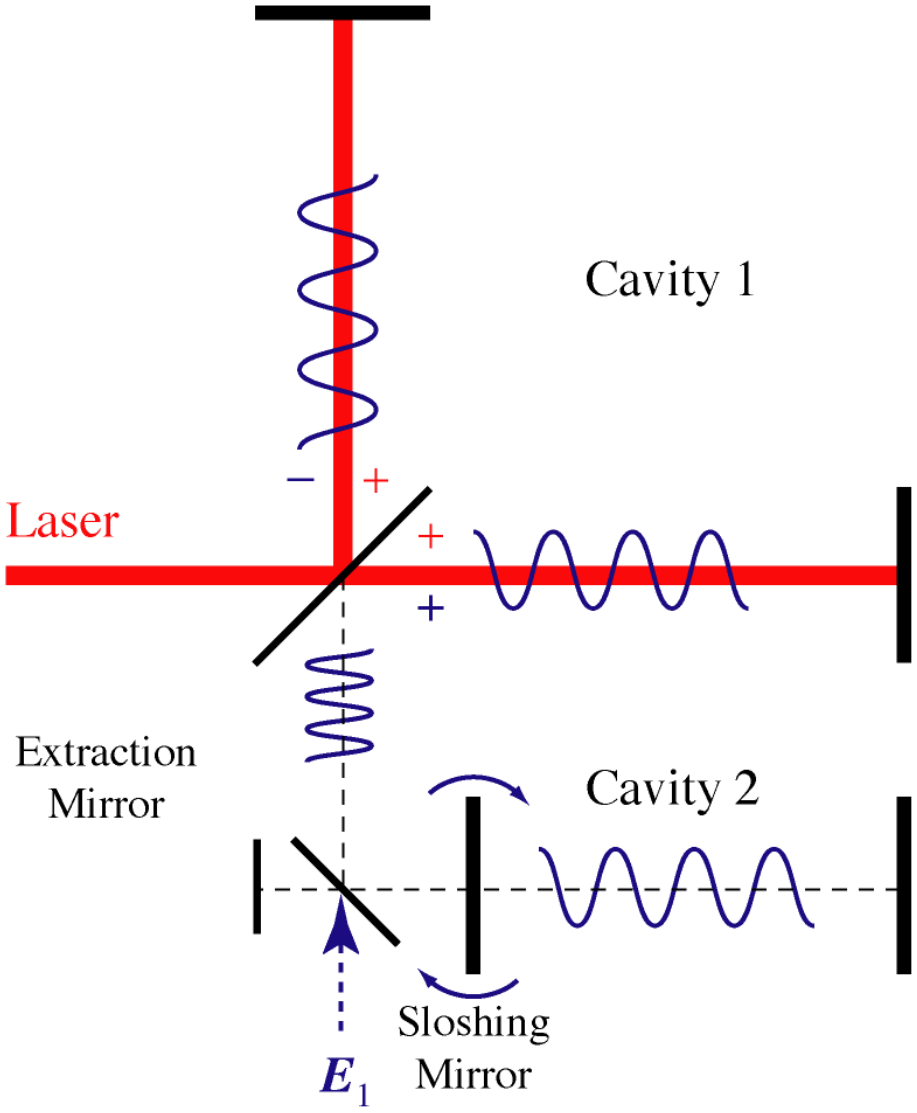

Figure 8: Diagram of a long SRC used as a Sloshing Speed Meter (SSM)

As shown in Fig. 8, in an interferometer with a tuned long SR cavity, modulations to the carrier sloshes between the arm cavity and the SR cavity, at a frequency Δ.

When the sloshing frequency Δ is much higher than the signal-extraction frequency δ (the rate at which signal leaks out from the interferometer), the situation can be described as "double signal recycling", in which both sidebands $\omega_0 \pm \Delta$, instead of a single sideband as in the usual signal-recycling configuration, can resonate in the interferometer [2, 16].

On the other hand, when Δ is comparable to δ, the average sideband light only sloshes once before leaving the interferometer. In this case, since the sloshing adds a π phase shift to the sideband light when it returns, the interferometer behaves like a speed meter [17] — which had been sought for by the quantum-measurement community on grounds that speed is related to momentum, which for free mass is a so-called Quantum Non-Demolition (QND) observable [18, 21].

3.4 Multiple Carriers/Optical Springs

Although we have long used multiple RF sidebands in order to do the length and angle controls of the interferometer, the use of multiple carrier fields (i.e. multiple lasers) has not been fully explored as a means of improving the sensitivity. Using a low noise phase locking servo, we can in principle, synchronize 2 or more independent lasers and use them to read out the GW signal, the auxilliary degrees of freedom, and to modify the opto-mechanical dynamics of the interferometer.

3.4.1 Multiple carriers in the same interferometer

Examples of such schemes are:

- Double optical spring [33] stabilization of the optomechanical instability, and further optimizations of configurations in which both carriers enter the arm cavities resonantly.
- Local readout [34, 35] improving low-frequency sensitivity of Advanced LIGO, in which one of the carriers does not enter the arm cavity, but simply reads out the motion of the ITMs.
- Use of a high power sub-carrier, injected from the PSL. This secondary laser would be set at one of the Free-Spectral Range (FSR) of the Power Recycling Cavity (PRC) and the arm cavities, but would be detuned in the SRC with the opposite sign relative to the carrier. This extra field can be used to *cancel* the optical spring [11].

These schemes can, in general, employ alternative wavelength lasers. The advantage of choosing a sub-carrier with an offset frequency less than ~ 1 GHz, is that the phase locking can be done with conventional electronics and that the mirror reflectivities are basically unchanged for such small changes in wavelength.

3.4.2 Intracavity Readout scheme

This refers to configurations in which gravitational wave is detected when a second carrier field (or some other sensing device) is used to measure the motion of a particular set of mirrors in their local inertial frames (see Ref. [36] and references therein). The word "intracavity" is used because it was assumed that the first carrier field does not generate useful output signals for readout.

The "local readout scheme" mentioned in the previous subsection can be regarded as an example of a mixture of intra- and extra-cavity readout. In high frequencies, the interferometer is dominated by extra-cavity readout, while in lower frequencies, it is dominated by intra-cavity readout. In the local readout example above, one may find it useful to use an alternate wavelength laser: the second wavelength can be made to have a very high finesse in the recycling cavities only, so as to maintain a high phase sensitivity for the ITM motion.

3.5 Dual Band - Dual Interferometer

The trouble with making an interferometer with good low frequency sensitivity is often in the power handling:

- The radiation pressure torques require noisy angular control systems. Conversely, it is easy to design a very robust angular control system for a high frequency only interferometer.
- The high laser power deposits heat into the mirrors, complicating the design of cryogenic systems.
- Requiring low optical losses in mirror coatings overly restricts the design of low *mechanical* loss coatings.
- Technical and Quantum radiation pressure from high laser power produce excess displacement noise at low frequencies.

By having two interferometers per site, we can have a broadband sensitivity improvement. The high frequency interferometer can operate with modest seismic isolation, small mirrors, and MW scale arm cavity powers. The low frequency interferometer can be cryogenic, use heavy mirrors, use low thermal noise coatings, etc.

A similar solution has been outlined for the Einstein Telescope [37].

3.5.1 Suspension Point Interferometer

In a specialized case of the dual-band idea, the penultimate mass of the low frequency suspension chain serves as the test mass for the high frequency interferometer. In this scheme, the locking of the Penultimate Interferometer serves to isolate the Ultimate Interferometer from seismic noise. As has been pointed out by Aso [10] and others [46], the mechanical mismatch between the suspensions can limit this suppression. The initial LIGO experience has shown that we can achieve a 1% match with no special care, so probably we can assume 0.1% for 3rd generation systems.

This level of suppression would allow moving the seismic wall down to ~ 1 Hz. The number of technical advantages in operating from a highly stable platform are numerous and need not be listed here.

3.6 Ponderomotive Squeezing

Squeezing can be induced by mirror motion under radiation pressure — this is called ponderomotive squeezing. It has been more difficult than generating squeezing with nonlinear crystals, yet it may become more reliable and more flexible in the future. Currently a Ponderomotive Squeezing experiment is going on at MIT [39]. See Fig. 9 for a sample configuration.

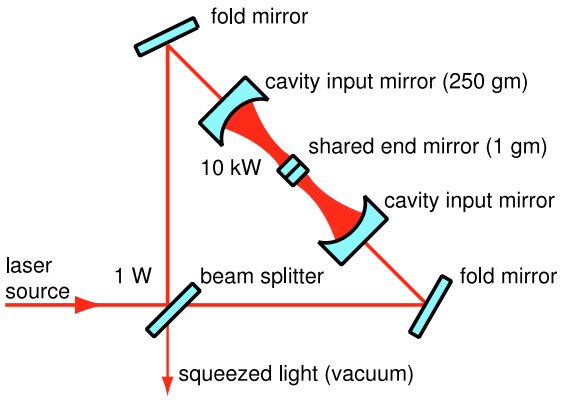

Figure 9: Ponderomotive Squeezer, taken from Corbitt et al. [38]

3.7 Atoms in Signal-Recycling Cavities

This is certainly a 3rd generation or beyond concept.

3.7.1 Internal squeezing and slow light

Previously, it was proposed [41] to use gratings to broaden the frequency response of the SRC. That approach has its problems. Another approach to a "white light" cavity is to use some kind of dispersive medium. Two approaches to this are to use a negative dispersion material [42] (such as an atomic vapor) and to use a photorefractive crystal [43].

In addition to its possible use in broadening the signal cavity, dispersive materials may have use in squeezing applications:

- Possibly, atomic clouds can be used as a form of squeezer in the SRC.
- It can slow down light, and possibly improve optical filters [40].

3.7.2 White-light cavity

Grating-based systems are shown to satisfy a rather general condition that $\partial\Phi/\partial\omega \geq 0$, which can also be connected with causality and conservation of probability [41] — how is this circumvented by the atom system?

3.7.3 Excess Noise

If atoms are to be inserted into interferometers, we must consider the excess noise induced by them. Since the main concern is with excess phase noise produced by the scatter, we should design and simulate the excess phase noise associated with these materials. The next step would be to demonstrate a higher optical phase sensitivity (increased signal without increased noise) at the $\sim 10^{-9}$ rad/$\sqrt{Hz}$ level.

3.8 Applications of Diffractive Gratings

Third generation.

3.8.1 All-reflective interferometers

Gratings can be used as beamsplitters in all-reflective interferometers [44]. These interferometers can potentially accommodate higher laser powers.

3.8.2 Alternative to multi-layer coatings

Gratings can be applied onto mirror surfaces to replace multi-layer dielectric gratings [45]

3.9 Significantly different configurations

For example, Displacement-Noise-Free Interferometry (DFI) [47]. Although DFI might turn out not to be suitable for ground-based detection, there might be new ideas in this vein.

3.10 General Questions

Theoretically, advanced gravitational-wave detectors have two limitations, the *Standard Quantum Limit* and the *Energetic Quantum Limit*.

- *Is SQL-beating unavoidable?* The SQL arises from a trade-off between back-action and sensing noise — and more fundamentally it arises from the fact that light in the interferometer couple to the positions of free masses, which cannot be measured continuously without additional noise. The SQL sets the scale at which radiation-pressure noise and optical spring become important. The SQL can be avoided if we avoid sensing back-action, using back-action-evasion techniques. It can also be circumvented if we have optical springs. It can fundamentally be eliminated if we have mirrors with infinite mass. However, Will heavy mirrors be available? Which is easier, heavy mirrors vs. light mirrors with SQL-beating?

- *Can we surpass the Energetic Quantum Limit?* The Energetic Quantum Limit arises from Energy-Phase uncertainty relation (see, e.g., [52]) and basically describes the requirement for higher optical power when lower shot noise is desired. This can in principle be surpassed by optical springs. However, optical spring frequency is usually low, and does not reach frequencies in which shot noise dominate. However, can one do something to make it work? What about very light test masses coupled with heavy test masses, something like the optical-lever scheme?

4 Macroscopic Quantum Mechanics with LIGO

Interferometers with classical noise budgets below the free-mass Standard Quantum Limit can be used to prepare (via cold-damping, radiation damping, or state collapse), evolve (in

	GW detection	MQM
optical spring	resonant enhancement in sensitivity	trapping and cooling of mirrors
back-action evasion	applied in steady state avoid back-action noise	applied in transient improves state tomography
signal processing techniques	extract signals	obtain conditional mirror states in real time
control system	(hold device at operation point)	cold-damping state preparation
squeezing	suppress noise	flexibility in state preparation better sensitivity in state tomography
non-Gaussian optical states	(no applications yet)	prepare highly non-classical mirror states

Table 1: Corresponding roles played by the same techniques in improving GW sensitivity and in exploring macroscopic quantum mechanics.

an optical-spring-induced potential well), and verify quantum states (through tomography) of macroscopic mirrors.

Techniques used to improve gravitational-wave sensitivity find corresponding roles in macroscopic quantum mechanics experiments, as shown in Table 1.

A Mirror shape and composition

Thermal noise of the substrate and coating may be lowered if we consider mirror substrates and coatings with unconventional shapes and composition. On the other hand, in the quest for mirrors with large masses, we may have to consider composite mirrors made up from a smaller mirror with high optical and mechanical quality, but with the remaining part connected to the high-quality part in such a way that the total thermal noise and optical loss do not increase significantly.

A.1 Non-TEM$_{00}$ modes

Three types of alternatives to fundamental TEM(0,0) modes have been considered, as summarized in table 2, also see the review article [48].

A.1.1 Higher Order Laguerre-Gauss Modes

The most straightforward way to improve thermal noise is to use higher-order Laguerre-Gauss (LG) modes of cavities with spherical mirrors [7, 8]. These modes naturally have broader, and more uniform coverage over the mirror surface. There is no need to modify the shape of the mirrors, although mirror radii of curvature should be adjusted (toward the *less degenerate* direction) in order that the higher LG modes now have the same loss as the fundamental LG(0,0) mode used to have. Experimental tests generating and resonating LG33 modes in a short cavity has also been carried out [9].

These modes are intrinsically degenerate – and therefore may cause complications when being attempted. We need to consider

- Whether we need to break the degeneracy intentionally, making the operating mode of the interferometer enough non-degenerate?
- Will the mode degeneracy be split naturally by figure errors in the polishing or the astigmatism caused by the gravitational sag?
- Can "corrective coatings" be used to intentionally "de-figure" the mirror surface?
- Can the outer ring of a composite test mass be used to apply stresses *in situ* to deform the mass and avoid unforseen degeneracies?
- How far out of the cavity linewidth do the higher order modes have to be split?

A.1.2 Modes supported by non-spherical mirrors

Mesa Beams. An *ad hoc* construction of optical modes that have lower thermal noise was to superimpose minimal Gaussian modes (i.e., those with waist at the center of the cavity and minimum spot size at the position of mirrors), with their symmetry axes either translated or rotated, to form a new mode with broader intensity profile at the mirrors. This resulted in the so-called Mesa beams, which are supported by Mexican-Hat mirrors [49].

Mode	Mirror Shape	Coating Noise Suppression Factor	Advantage	Disadvantage
LG(3,3)	Spherical	1.61	Spherical Mirrors	Degeneracy
Mesa	Mexican-Hat	1.53	Simple Construction	non-spherical mirrors
Optimal	Conical	2.30	Low Noise	non-spherical mirrors

Table 2: Alternative Optical Modes that have been considered for use in GW detectors, mirror shapes that support them, and their coating-thermal-noise suppression factors (in Advanced LIGO situation, namely 4 km arm length and 17 cm mirror radius).

Beam with minimum thermal noise. Work has been done to optimize over all optical modes with $m = 0$, and search for the mode with minimum coating thermal noise, keeping the same diffraction loss [50]. For a pure $m = 1, 2, 3$ modes, explorations show that only slight improvements can be made [51].

Further optimization. For reference, an unreachable (due to diffraction) theoretical upper limit of coating thermal-noise improvement can be obtained by assuming a uniform power profile, which is a factor 2.63 below the baseline Gaussian mode, or a factor 1.14 below the $m = 0$ optimal mode. This means additional optimization regarding thermal noise alone may not be possible. However, the beam with minimum thermal noise is shown to be very sensitive to mirror figure error. A subject of further research is to jointly optimize for coating noise and tolerance to mirror figure error.

Practical issues with non-sperical mirrors. Non-spherical mirrors, although can achieve lower thermal noise in theory, have not been used in high precision laser interferometry. We need to consider the following issues:

- Difficulty in manufacturing.
- Higher susceptibility to figure errors
- Difficulty in locking, and more stringent requirements on tilt and translation control.
- May require non-spherical mirrors for all input-output optics, e.g., mode cleaners, squeezers, etc.

A.2 Multi-Layer Coating designs

Coating Brownian noise might be lowered by altering the structure of the multi-layer dielectric coating. This will require further modeling of correlations in the coating taking into account anisotropic losses and, at least, a 2D model (cylindrical symmetry).

A.3 Composite Mirrors

Several (force) noise sources can be reduced by increasing the mass of the mirrors. It seems difficult to produce high quality mirrors with more than 100 kg mass. To reap the rewards of increased mass without producing larger mirrors, it may be possible to produce a heavy *composite* mirror.

A.3.1 Composite Mass

Purely as an example, one can imagine encasing the central (high quality) mirror with an outer donut shape made of low optical quality, but moderately high mechanical quality material. For example, the inner mirror could be a 100 kg fused silica of high Q and the outer donut can be a fused quartz ring. The interface can be made by a thin sheet of indium or gold. Of course, one would have to take appropriate care not increase the thermal noise.

Another example would be to do as above, but have the contacts be only at the points where the *ears* are on the existing mirrors. In this way, the thermal noise penalty is only as bad as the existing 2nd generation suspensions.

A.3.2 Cavity/Etalon based

Two mirrors separated along their common optical axis, e.g., the Khalili cavity. Can we also combine this into the "optical configuration"?

B Suspension Thermal Noise

The dominating noise source in the 10-40 Hz band would be the pendulum mode thermal noise of the monolithic fused silica suspension (c.f. Figure 1). Around ∼12 Hz, the thermal noise of the bounce mode of the monolithic stage dominates.

For the GWINC-based model used here to evaluate optical topologies, we have assumed an improved suspension configuration:

1. Cryogenically cooled (20K) Silicon fibers for the link between the PUM and test mass.
2. 4K Silicon blade springs at the PUM stage to reduce the vertical mode frequency.

This is not a suspension design, just a concept. Its likely that there will be major problems with trying to operate a suspension which such a large thermal gradient on its ears.

For more details and discussions, see Sections 2.2 and 2.3 of the ISG White Paper.

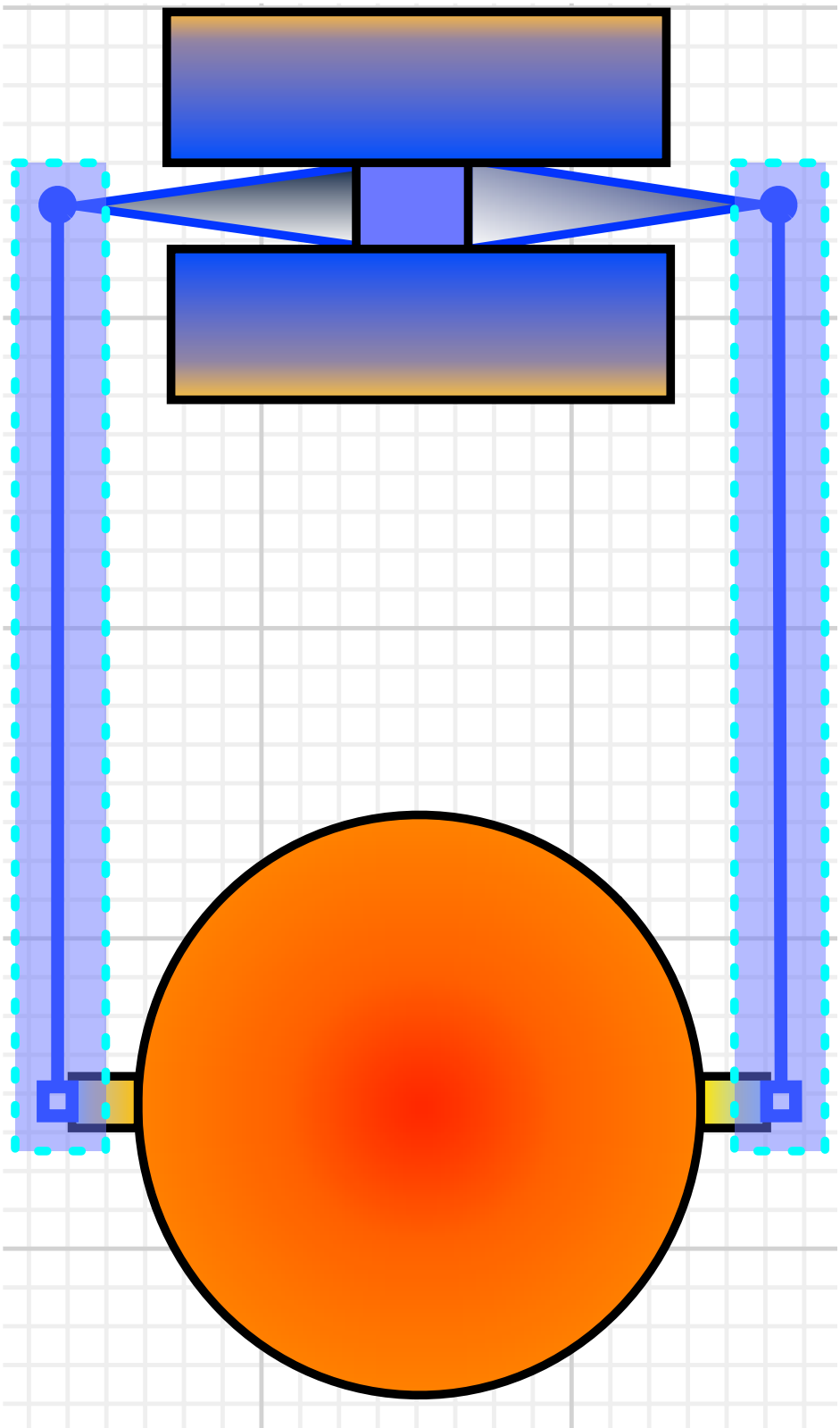

Figure 10: PUM cooled by conduction with 4K OFC copper braids. Si fiber cooled conductively via blades and radiatively by noncontacting radiative shield.

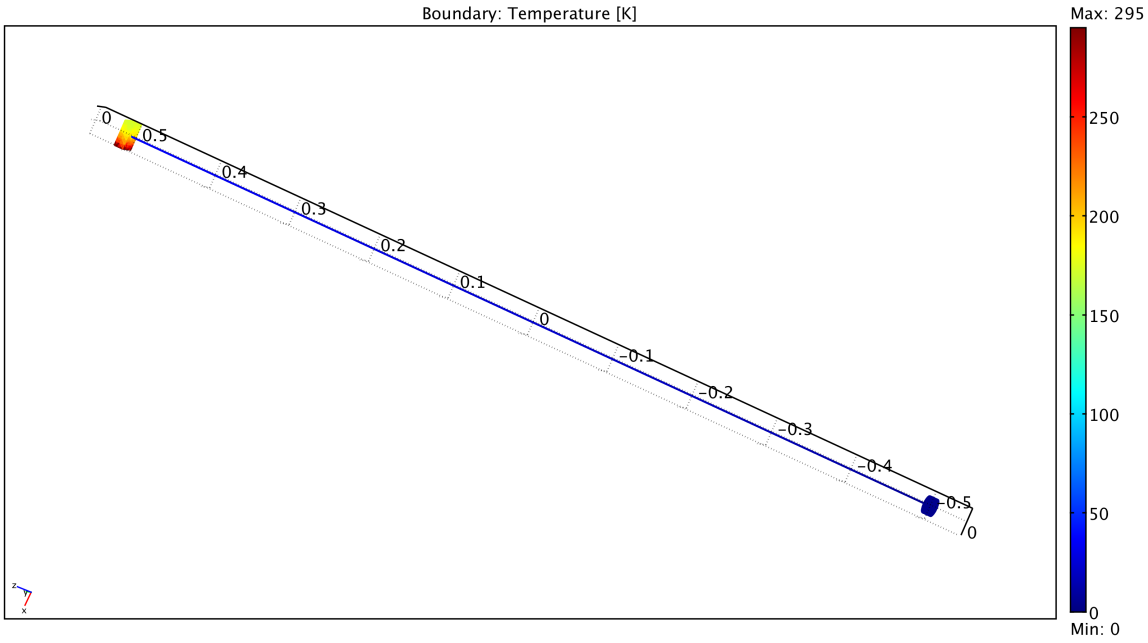

Figure 11: COMSOL model of fiber.

C Straw-man configurations for LIGO2.5

In this section, we present two straw-man optical configurations for LIGO 2.5, which assumes the classical-noise improvement cited in Sec. 2.1, and have broadband sensitivity. These have all been calculated using a development version of GWINC [4] called GWINCDEV.

1. Frequency dependent input squeezing (IS for short)
2. Frequency independent squeezing and output filtering (VO for short)

We list the parameters used in these configurations in Table 3, and plot their noise spectra in Fig. 12.

parameter	value
arm-cavity circulating power	730 kW
arm-cavity bandwidth	43 Hz
signal bandwidth (after RSE)	700 Hz
arm-cavity round-trip loss	100 ppm
photodetection efficiency	99%
filter loss per round trip	3 – 100 ppm
filter length	100 m
input squeeze factor	10 dB
squeezing injection loss	5%
test mass' mass	100 kg

Table 3: Parameters assumed for Straw-man configurations

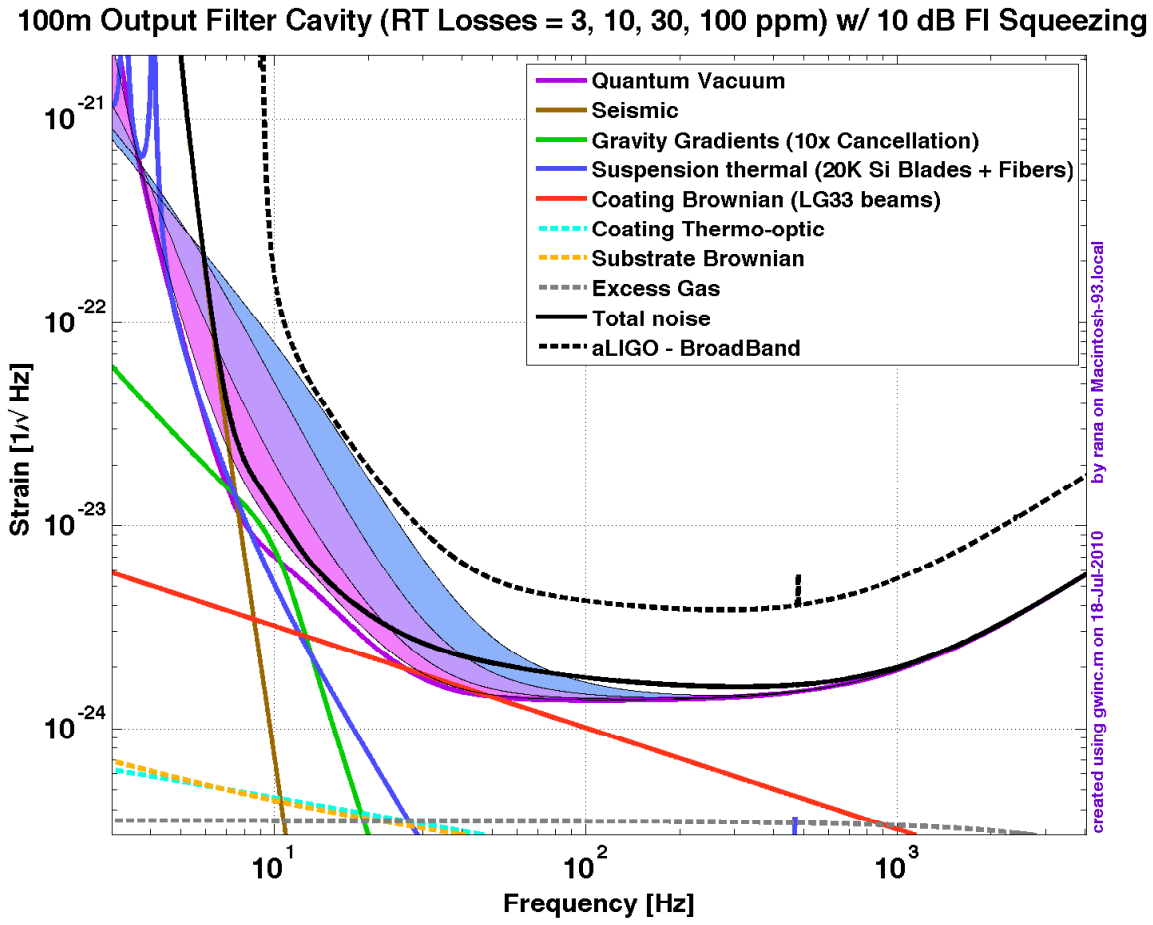

Figure 12: Noise spectrum using 10 dB of squeezing injection and a 100 m variational output filter cavity. The shaded regions indicate the low frequency quantum noise spectrum assuming RT losses of 3, 10, 30, & 100 ppm in the output filter cavity.

References

[1] Y. Pan, "Black Holes and Signal Recycling Cavities", Caltech PhD. thesis, 2007

[2] J. Mizuno, "Comparison of optical configurations for laser-interferometric gravitational-wave detectors", Univ. of Hannover, 1995

[3] R. Weiss, "Electromagnetically Coupled Broadband Gravitational Antenna", http://www.ligo.caltech.edu/docs/P/P720002-01

[4] LIGO, "GWINC Wiki", http://ilog.ligo-wa.caltech.edu:7285/advligo/GWINC

[5] M. Evans, "Optickle", http://www.ligo.caltech.edu/docs/T/T070260-00.pdf

[6] P. Fritschel, "LIGO", http://arxiv.org/abs/0711.3041

[7] B. Mours, E. Tournefier, and J.-Y. Vinet, Class. Quantum Grav. **23**, 5777 (2006).

[8] S. Chelkowski, S. Hild, A. Freise, "Prospects of higher-order Laguerre-Gauss modes in future gravitational wave detectors", http://link.aps.org/doi/10.1103/PhysRevD.79.122002

[9] Paul Fulda, Keiko Kokeyama, Simon Chelkowski and Andreas Freise, "Experimental demonstration of higher-order Laguerre-Gauss mode interferometry", http://arxiv.org/abs/1005.2990

[10] Y. Aso, "Stabilization of a Fabry-Perot Interferometer using a Suspension Point Interferometer", Phys. Lett. A (2004) http://dx.doi.org/10.1016/j.physleta.2004.04.066

[11] H. Yang, H. Miao, Y. Chen and R. Adhikari, "Wideband sub-SQL Interferometer for GW Detection", in prep., 2010

[12] D. Sigg and J. Sidles, "Optical Torques in Suspended Fabry-Perot Cavities", http://www.ligo.caltech.edu/docs/P/P030055-C/

[13] R. Adhikari, "Sensitivity and Noise", http://www.ligo.caltech.edu/docs/P/P040032-00.pdf

[14] ISC Group, "Interferometer Sensing and Control Requirements", http://www.ligo.caltech.edu/docs/T/T070236-00.pdf

[15] G. de Vine, D.A. Shaddock and D.E. McClelland, "Variable reflectivity signal mirrors and signal response measurements", Class. Quantum Grav. **19** 1561 (2002).

[16] A. Thuering, R. Schnabel, H. Lueck and K. Danzmann, "Detuned Twin-Signal-Recycling for ultra-high precision interferometers," Opt. Lett. **32**, 985-987 (2007).

[17] P. Purdue and Y. Chen, "Practical speed meter designs for quantum nondemolition gravitational-wave interferometers", Phys. Rev. D **66** 122004 (2002).

[18] P. Purdue, "Analysis of a quantum nondemolition speed-meter interferometer," Phys. Rev. D **66**, 022001 (2002).

[19] G. Rempe, R. Thompson, H. J. Kimble and R. Lalezari, "Measurement of Ultra Low Losses in an Optical Interferometer", Optics Letters (1992)

[20] N. Uehara, A Ueda, K Ueda, H Sekiguchi, T Mitake "Ultralow-loss mirror of the parts-in $10^{-}6level at 1064nm''OpticsLetters(1995)$

[21] V.B. Braginsky, M.L. Gorodetsky, F.Y. Khalili, K.S. Thorne, "Dual-resonator speed meter for a free test mass," Phys. Rev. D **61** 044002 (2000).

[22] W.G. Unruh, in Quantum Optics, Experimental Gravitation, and Measurement Theory, edited by P. Meystre and M.?O. Scully (Plenum, New York, 1983), p. 647.

[23] C.M. Caves, Phys. Rev. D **23**, 1693 (1981).

[24] S.P. Vyatchanin and A.B. Matsko, JETP **77**, 218 (1993);S. P. Vyatchanin and E.A. Zubova, Phys. Lett. A **203**, 269 (1995);ibid.S.P. Vyatchanin, **239**, 201 (1998).

[25] H.J. Kimble et al., "Conversion of conventional gravitational-wave interferometers into quantum nondemolition interferometers by modifying their input and/or output optics", Phys. Rev. D **65** 022001 (2001).

[26] J. Harms, Y. Chen, S. Chelkowski, et. al., "Squeezed-input, optical-spring, signal-recycled gravitational-wave detectors", Phys. Rev. D **68**, 042001 (2003).

[27] A. Buonanno and Y. Chen, "Improving the sensitivity to gravitational-wave sources by modifying the input-output optics of advanced interferometers ", Phys. Rev. D **69** 102004 (2009).

[28] T. Corbitt, N. Mavalvala and S.E. Whitcomb, "Optical cavities as amplitude filters for squeezed fields", Phys. Rev. D **70**, 022002 (2004).

[29] F.Ya. Khalili, "Increasing future gravitational-wave detectors sensitivity by means of amplitude filter cavities and quantum entanglement", Phys. Rev. D **77**, 062003 (2008).

[30] F.Ya. Khalili, H. Miao and Y. Chen, "Increasing the sensitivity of future gravitational-wave detectors with double squeezed-input", Phys. Rev. D **80**, 042006 (2009).

[31] R. Adhikari, LIGO Document, LIGO-G-1000524 (2010).

[32] D.L. Danilishin and F.Ya. Khalili, Phys. Lett. A **300** 547-558 (2002).

[33] H. Rehbein, H. Müller-Ebhardt, K. Somiya et al., "Double optical spring enhancement for gravitational-wave detectors", Phys. Rev. D **78**, 062003 (2008).

[34] H. Rehbein, H. Müller-Ebhardt, K. Somiya et al., "Local readout enhancement for detuned signal-recycling interferometers", Phys. Rev. D **76**, 062002 (2007)

[35] J.-M. Courty, A. Heidmann, and M. Pinard, "Quantum Locking of Mirrors in Interferometers", Phys. Rev. Lett. **90**, 083601 (2003).

[36] S.L. Danilishin and F.Ya. Khalili, "Practical design of the optical lever intracavity topology of gravitational-wave detectors", Phys. Rev. D **73**, 022002 (2006).

[37] S. Hild, S. Chelskowski, A. Freise, et al., "A Xylophone Configuration for a third Generation Gravitational Wave Detector", Class. Quantum Grav. **27**, 015003 (2010).

[38] T. Corbitt, Y. Chen, N. Mavalvala, "Mathematical framework for simulation of quantum fields in complex interferometers using the two-photon formalism", Phys. Rev. A **72**, 013818 (2005).

[39] T. Corbitt, Y. Chen, F.Ya. Khalili, et al., "Squeezed-state source using radiation-pressure-induced rigidity", Phys. Rev. A **73**, 023801 (2006).

[40] E.E. Mikhailov, K. Goda, T. Corbitt, and N. Mavalvala, "Frequency-dependent squeeze-amplitude attenuation and squeeze-angle rotation by electromagnetically induced transparency for gravitational-wave interferometers", Phys. Rev. A **73**, 053810 (2006).

[41] S. Wise, V. Quetschke, A.J. Deshpande, et al., "Phase Effects in the Diffraction of Light: Beyond the Grating Equation", Phys. Rev. Lett. **95**, 013901 (2005).

[42] G. S. Pati, et. al., "Demonstration of a Tunable-Bandwidth White-Light Interferometer Using Anomalous Dispersion in Atomic Vapor", Phys. Rev. Lett. (2007)

[43] H. N. Yum, et. al. "Fast-light in a photorefractive crystal for gravitational wave detection", Opt. Express (2008)

[44] K.-X. Sun and R.L. Byer, "All-reflective Michelson, Sagnac, and Fabry-Perot interferometers based on grating beam splitters", Opt. Lett. **23** 567 (1998); J. Hallam et al., "Coupling of lateral grating displacement to the output ports of a diffractive Fabry-Perot cavity", arXiv:0903.3324; A. Freise, A. Bunkowski and R. Schnabel, "Phase and alignment noise in grating interferometers", New J. Phys. **9**:433 (2007).

[45] A. Bunkowski, "High reflectivity grating waveguide coatings for 1064nm", Class. Quant. Grav. **23**:7297-7304 (2006).

[46] A. Freise, et. al., "Optical Detector Topology for Third Generation Gravitational wave Observatories", `http://arxiv.org/abs/0908.0353v2`

[47] S. Kawamura and Y. Chen, "Displacement-Noise-Free Gravitational-Wave Detection " , Phys. Rev. Lett. **93** 211103 (2004).

[48] Jean-Yves Vinet, "On Special Optical Modes and Thermal Issues in Advanced Gravitational Wave Interferometric Detectors", Living Rev. Relativity 12, (2009), 5. URL (cited on July 11,2010): `http://www.livingreviews.org/lrr-2009-5`

[49] E. D'Ambrosio et al., "Reducing Thermoelastic Noise in Gravitational-Wave Interferometers by Flattening the Light Beams", arXiv:gr-qc/0409075 (2004); M. Bondarescu and K.S. Thorne, "New family of light beams and mirror shapes for future LIGO interferometers", Phys. Rev. D **74**, 082003 (2006); A.P. Lundgren, R. Bondarescu, D. Tsang, and M. Bondarescu, "Finite mirror effects in advanced interferometric gravitational wave detectors", Phys. Rev. D **77**, 042003 (2008).

[50] M. Bondarescu, O. Kogan and Y. Chen,"Optimal light beams and mirror shapes for future LIGO interferometers," Phys. Rev. D **78**, 082002 (2008).

[51] Z. Zhang, unpublished (2010).

[52] V.B. Braginsky, M.L. Gorodetsky, F.Ya. Khalili and K.S. Thorne, "Energetic Quantum Limit in Large-Scale Interferometers," arXiv:gr-qc/9907057v2 (1999).